Organic Mixed Ionic-Electronic Conductors Based on Tunable and Functional Poly(3,4-ethylenedioxythiophene) Copolymers

Wu, Jiaxin; Gu, Modi; Travaglini, Lorenzo; Lauto, Antonio; Ta, Daniel; Wagner, Pawel; Wagner, Klaudia; Zeglio, Erica; Savva, Achilleas; More Authors

DOI
10.1021/acsami.4c03229

Publication date
2024

Document Version
Final published version

Published in
ACS Applied Materials and Interfaces

ACS APPLIED MATERIALS & INTERFACES

www.acsami.org

Research Article

Organic Mixed Ionic–Electronic Conductors Based on Tunable and Functional Poly(3,4-ethylenedioxythiophene) Copolymers

Jiaxin Wu, Modi Gu, Lorenzo Travaglini, Antonio Lauto, Daniel Ta, Pawel Wagner, Klaudia Wagner, Erica Zeglio, Achilleas Savva, David Officer, and Damia Mawad*

Cite This: https://doi.org/10.1021/acsami.4c03229

Read Online

ACCESS | Metrics & More | Article Recommendations | Supporting Information

ABSTRACT: Organic mixed ionic–electronic conductors (OMIECs) are being explored in applications such as bioelectronics, biosensors, energy conversion and storage, and optoelectronics. OMIECs are largely composed of conjugated polymers that couple ionic and electronic transport in their structure as well as synthetic flexibility. Despite extensive research, previous studies have mainly focused on either enhancing ion conduction or enabling synthetic modification. This limited the number of OMIECs that excel in both domains. Here, a series of OMIECs based on functionalized poly(3,4-ethylenedioxythiophene) (PEDOT) copolymers that combine efficient ion/electron transport with the versatility of post-functionalization were developed. EDOT monomers bearing sulfonic (EDOTS) and carboxylic acid (EDOTCOOH) groups were electrochemically copolymerized in different ratios on oxygen plasma-treated conductive substrates. The plasma treatment enabled the synthesis of copolymers containing high ratios of EDOTS (up to 68%), otherwise not possible with untreated substrates. This flexibility in synthesis resulted in the fabrication of copolymers with tunable properties in terms of conductivity (2–0.0019 S/cm) and ion/electron transport, for example, as revealed by their volumetric capacitances (122–11 F/cm^3). The importance of the organic nature of the OMIECs that are amenable to synthetic modification was also demonstrated. EDOTCOOH was successfully post-functionalized without influencing the ionic and electronic transport of the copolymers. This opens a new way to tailor the properties of the OMIECs to specific applications, especially in the field of bioelectronics.

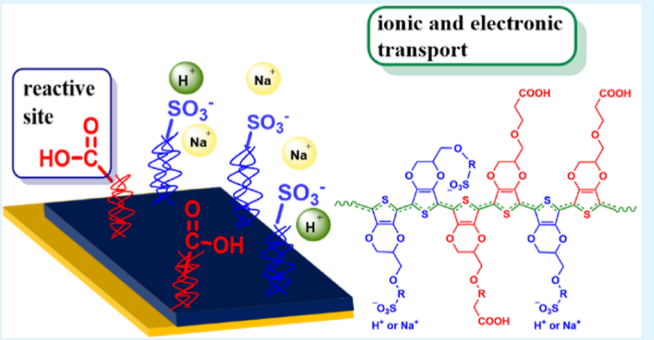

KEYWORDS: *PEDOT, self-acid-doping, copolymer, mixed ionic–electronic conductor, OMIEC*

1. INTRODUCTION

Organic mixed ionic–electronic conductors (OMIECs), of which conjugated polymers are the most prevalent, couple ionic and electronic transport within their bulk, a characteristic that makes them relevant to a range of applications including bioelectronics,[1] biosensors,[2] and neuromorphic computing.[3] Their organic nature is a key feature not only for providing a high free volume that facilitates the diffusion of ionic species in and out of the bulk of the material but also for enabling synthetic modification to tailor their properties. This has been recently demonstrated by the development of an azide-functionalized PEDOT homopolymer[4] that could be surface modified with proteins and enzymes without losing its high performance as an OMIEC in an organic electrochemical transistor (OECT) that relies on ion injection from the electrolyte. However, most of the literature on the development and optimization of OMIECs focuses on only one of these two features: tuning ion conduction or synthetic and post-functionalization. Here, we present a design strategy for OMIEC copolymers that combines both characteristics: efficient ion/electron transport with chemical handles that enable post-functionalization. We show that copolymerization offers flexibility in chemical composition and tunability of properties.

In an OMIEC, electronic conductivity is provided by the doped conjugated backbone of the polymer, while ionic conductivity is provided either by a polar group in the backbone or an ionized or polar entity blended or chemically linked to the polymer backbone.[5] The most prominent OMIEC is poly(3,4-ethylenedioxythiophene):poly(styrenesulfonate) (PEDOT:PSS), where PSS is a negatively charged polyelectrolyte blended with PEDOT, resulting in its doping. The polar polymer electrolyte poly(ethylene oxide) (PEO) has been blended with conjugated polymers such as poly(3-hexylthiophene) (P3HT)[6] and poly[2-methoxy-5-(2′-

Received: February 26, 2024
Revised: May 9, 2024
Accepted: May 15, 2024

ethylhexyloxy)-1,4-phenylenevinylene],[7] enabling ionic transport in addition to their intrinsic electronic transport. An alternative to blending is to copolymerize a polyelectrolyte or a polymer electrolyte with the conjugated polymer forming OMIEC block copolymers such as P3HT-*b*-PEO[8] and P3HT-*b*-PSS.[9] Homopolymers of sulfonic-modified PEDOT[10,11] and glycol-[12,13] or sulfonic-modified polythiophene[14] are examples of OMIECs in which the conjugated polymer has been modified with side chains that are ionized or polar in nature, aiding ion solvation. More recently, OMIEC copolymers based on ionized and nonionized conjugated precursors have been developed, such as copolymers of sulfonated thiophene with 3-hexylthiophene (PTHS-*co*-P3HT)[15] or sulfonated EDOT with nonfunctionalized EDOT (PEDOTS-*co*-PEDOT).[16,17] Other strategies to tune ionic conductivity include the use of small-size additives such as zonyl or dimethyl sulfoxide,[18] as well as changing environmental conditions such as humidity.[19,20]

These approaches have been shown to be effective in enhancing the ion transport of the conjugated polymer without impacting its electronic conductivity. However, while harnessing and optimizing the mixed ionic/electronic transport in the OMIEC is critical, it is equally important to take advantage of the versatile nature of its components, which, if chosen carefully, can enable post-modification to tailor the properties of the OMIEC for a particular application. This is no more relevant than in the case of bioelectronics, where surface engineering is often required to enhance integration of the device at the biotic interface. For example, an implantable bioelectronic device should feature an antifouling surface that reduces protein adsorption and minimizes the inflammatory response, thus, ensuring its electronic longevity. Zwitterionic moieties tethered on the surface of the implant have been shown to be an effective antifouling strategy.[21] Similarly, an OMIEC used in regenerative medicine applications would benefit from cell adhesion sites that promote cell integration and proliferation.[22] In sensing applications such as biomolecule or electrochemical detection where an OECT device configuration plays a role,[2] surface engineering is applied to prevent nonspecific binding and enhance the selectivity and specificity of the sensor.[23] Post-functionalization of the conjugated polymer rather than its precursor monomer is favorable owing to the large size of biological molecules, such as proteins, that can impede the polymerization process. Also, these biological moieties are commonly sensitive to the harsh conditions of the polymerization conditions.[24]

Polyelectrolytes such as PSS or polymer electrolytes such as PEO do not provide chemical handles for post-modification. Similarly, modifying the conjugated polymer itself with ionized or glycolated side chains does not enable synthetic flexibility and neither does its copolymerization with polymers that bear no functional groups. Blending the conjugated polymer with an insulating polymer that bear functional groups such as carboxymethylated dextran[25] or poly(vinyl alcohol)[26] has been demonstrated to be an effective strategy for the covalent functionalization of the conductive surface;[27] however, the long-term physical stability of the composite needs to be considered as it is likely that the blended polymer can leach out as swelling occurs over time. Homopolymers based on thiophene or EDOT monomers bearing reactive functional groups such as maleimide,[28] boronic acid,[29] azide,[30] hydroxyl,[31,32] and carboxylic groups[33,34] have been successfully synthesized. While these synthetic designs enable post-functionalization of the reactive functional groups,[24] homopolymers do not permit flexibility in tuning the material's properties. A solution to this would be an organic semiconductor copolymer that bears reactive functional groups for post-functionalization and polar/ionized groups for enhanced ion transport. Functional monomers have been used in the synthesis of conjugated copolymers, with examples including copolymerization of EDOT with EDOT bearing a carboxylic group[35] or a thioacetate.[36,37] However, these copolymers lack the ionized or polar component that enhances the ion conductivity in the OMIEC.

We were the first to demonstrate the synthesis of an electropolymerized PEDOT-based copolymer bearing equimolar ratios of EDOT monomers modified with uncapped ionized sulfonate groups (EDOTS) and reactive carboxylic acid functional groups (EDOTCOOH).[38] We showed that electropolymerization is a straightforward time-efficient synthetic method to produce a copolymer that is stable and electroactive in an aqueous electrolyte, with significantly enhanced ion and electron conductivity compared to a homopolymer composed only of EDOTCOOH. A similar copolymer based on EDOTS and EDOT bearing a reactive hydroxysuccinimide group was then synthesized by direct (hetero)arylation polymerization, resulting in a copolymer (PEDOT-NHS) that is conductive and could be post-functionalized with gelatin.[39] These studies demonstrated that copolymerization of monomers functionalized with ionized and reactive functional groups is a valid synthetic strategy for the development of OMIECs with efficient electron and ion transport, while capitalizing on their potential for post-functionalization.

Here, we present a series of OMIEC copolymers with varied ratios of EDOTS and EDOTCOOH synthesized on oxygen-plasma-treated conductive substrates. We show that the plasma treatment enables the synthesis of copolymers with increased ratios of EDOTS in comparison to EDOTCOOH, ensuring that the copolymer films do not delaminate and thus facilitate electrochemical characterization. This was not feasible in our previous work that was based on untreated working electrodes.[38] Films with increased EDOTS ratios in the copolymer synthesized on untreated substrates delaminated under electrochemical characterization. We adopt electrochemical polymerization for the synthesis of the copolymers due to the simplicity of this technique that requires no catalyst or organic solvents, is time efficient with the reaction completed in a few minutes, and affords the fabrication of the copolymer film directly on the required substrate, eliminating further processing steps. We show that oxygen plasma treatment of the conductive substrates enables the electropolymerization of copolymers with varied chemical composition. We also demonstrate that by controlling the chemical composition of the copolymers, properties of the OMIECs such as morphology, conductivity, and ion and electron transport can be varied and improved compared to our previously reported poly(EDOTS-*co*-EDOTCOOH). Finally, we surface-functionalize the copolymers, taking advantage of the tethered carboxylic groups, and show that post-functionalization does not affect the electrochemical properties of the OMIEC. The field has been dominated with material designs focused on homopolymers that either excel as efficient ion/electron conductors or functional materials that enable post-modification. Similarly, blending of the OMIEC with insulating polymers bearing functional side groups for post-modification has been equally important to achieve tailored bioelectronic

https://doi.org/10.1021/acsami.4c03229
ACS Appl. Mater. Interfaces XXXX, XXX, XXX−XXX

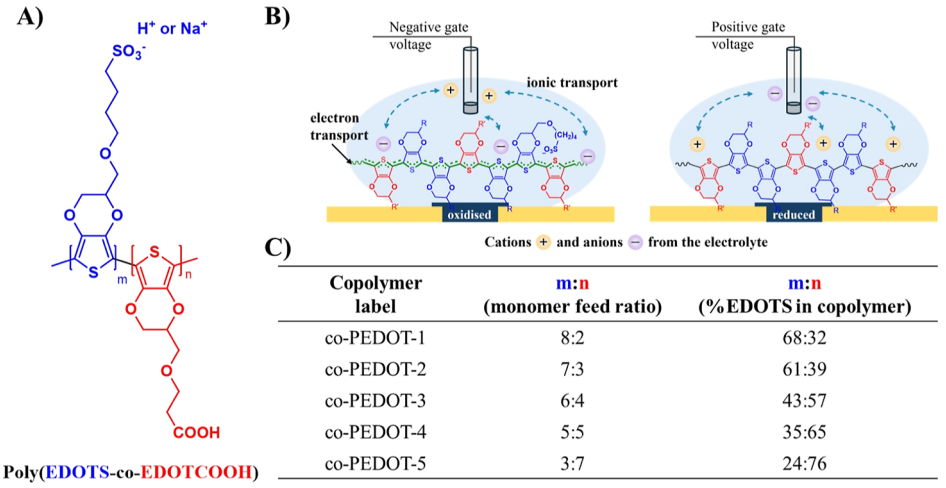

C)

Copolymer label	m:n (monomer feed ratio)	m:n (% EDOTS in copolymer)
co-PEDOT-1	8:2	68:32
co-PEDOT-2	7:3	61:39
co-PEDOT-3	6:4	43:57
co-PEDOT-4	5:5	35:65
co-PEDOT-5	3:7	24:76

Figure 1. (A) Chemical structure of the copolymer poly(EDOTS-*co*-EDOTCOOH). (B) Scheme illustrating the ionic/electronic transport mechanism in the copolymer films when in contact with an electrolyte and under an applied voltage. (C) Labels of copolymer films synthesized with varying monomer feed ratios and % of EDOTS in the copolymer films quantified from the XPS data.

surfaces. Our design of conjugated copolymers that integrate efficient ionic/electronic transport and post-functionalization and can be synthesized in a time-efficient, one-step procedure with tuned chemical compositions is a key advance for tailoring bioelectronics to various bioapplications.

2. EXPERIMENTAL SECTION

2.1. Materials. 3-[(2,3-Dihydrothieno[3,4-*b*][1,4] dioxin-2-yl)-methoxy] propanoic acid (EDOTCOOH)[34,40] and sodium 4-[(2,3-dihydrothieno[3,4-*b*][1,4]dioxin-2-yl)methoxy]butane-1-sulfonate (EDOTS)[16] were synthesized according to the literature. Sodium hydroxide (NaOH), hydrochloric acid (HCl), lithium perchlorate ($LiClO_4$), 2-(*N*-morpholino)ethanesulfonic acid (MES buffer), *N*-hydroxysuccinimide (NHS), 1-ethyl-3-(3-(dimethylamino)propyl)-carbodiimide (EDC), *N*-(3-aminopropyl)-2-methylacrylamide hydrochloride (1:1) (APMA), sodium hydrogen carbonate ($NaHCO_3$), phosphate-buffered saline (PBS) tablets, sodium chloride (NaCl), ammonium hydroxide (NH_4OH), and hydrogen peroxide (H_2O_2) were purchased from Sigma-Aldrich and used with no further purification.

2.2. Electropolymerization of Copolymer Films. Different formulations with varied feed ratios of EDOTS to EDOTCOOH (Figure 1 and Table S1) were prepared by electropolymerization on a plasma-treated indium tin oxide (ITO)-coated substrate, an interdigitated microelectrode (IDME, Micrux Technologies, length L = 10 μm, width w = 50 cm), or a single channel device having two gold electrodes (length L = 30 μm, width w = 1 mm). Prior to use, the substrates were cleaned using a mixture of ammonium hydroxide, hydrogen peroxide, and water (NH_4OH/H_2O_2/deionized water = 1:1:5) for 5 min at 80 °C[41] and then treated with oxygen plasma (Diener Femto Model 4) for 6 min at 80 W. In a typical procedure to synthesize co-PEDOT-1 as an example, EDOTCOOH (0.048 mmol) was added to 2 mL of 0.2 M NaOH. The mixture was vortexed for 5 min to ensure EDOTCOOH was fully dissolved, followed by the addition of 2 mL of 0.2 M HCl to neutralize the excess of NaOH. EDOTS (0.192 mmol) and $LiClO_4$ (42.6 mg, 0.4 mmol) were then added to the EDOTCOOH solution, and the mixture was vortexed to fully dissolve the compounds. The pH of the solution was adjusted to 2 by adding 0.2 mL of 0.2 M HCl. The solution was then transferred to a glass Petri dish for the electrosynthesis of the copolymers by performing cyclic voltammetry (CV) under a voltage ranging from −0.6 V to +1.1 V, with a scan rate of 50 mV/s for 5 cycles (PGSTAT204 Autolab potentiostat). The reference and auxiliary electrodes used were an Ag/AgCl electrode and a platinum pad (10 × 12 × 1 mm), respectively. The working electrode was an ITO substrate for growing films used for X-ray photoelectron spectroscopy (XPS), contact angle spectroscopy, atomic force microscopy (AFM), CV, in situ spectroelectrochemistry, and electrochemical impedance spectroscopy. The IDME substrate was the working electrode used for growing the films to be characterized as channel materials in an OECT. The single-channel device was used as the working electrode for producing films for recording the current−voltage (I−V) curves. After electropolymerization, the working electrodes were taken out of the electrolyte solution and soaked in deionized water for 5 s to remove any excess electrolyte or unreacted monomers from the films. The onset potential (E_{onset}) for each formulation was calculated from the intersection of two tangent lines drawn at maximum and minimum currents.

2.3. Structural and Surface Morphology Characterization. *2.3.1. X-ray Photoelectron Spectroscopy.* XPS was used to determine the ratio of the two monomers, EDOTS and EDOTCOOH, in each copolymer film. A Thermo Scientific ESCALAB250Xi X-ray photoelectron spectrometer was used with AlK_α X-rays (E_{photon} = 1486.7 eV) and a 90° photoelectron takeoff angle. The spectra were recorded under a 100 eV pass energy between 0 and 1350 eV, and the elements (C 1s, O 1s, and S 2p) were measured with a 20 eV pass energy. The parameters of the elements for the spectrometer included C 1s (284.8 eV) for the binding energy (BE) for adventitious hydrocarbon, Cu $2p^3$ (932.6 eV), Ag $3d^5$ (368.2 eV), and Au $4f^7$ (84.0 eV). XPS peaks were deconvoluted using Origin software with Gaussian mode peak assignments. Assignments of the peaks are reported in Table S2. Quantitative analysis was performed on the S 2p spectra to calculate the % of EDOTS in the copolymers. The area under the curve corresponding to the sulfonic groups tethered on EDOTS was divided by the sum of the areas corresponding to the sulfur of the thiophene ring (neutral sulfur, oxidized sulfur, and sulfone).

2.3.2. Contact Angle. The surface wettability of the copolymer films was assessed by using a contact angle goniometer (Ossila Instruments) equipped with a camera. A drop of deionized water was dispensed vertically on the surface of the copolymer films and was left for 60 s before images were acquired. The contact angle (θ_e) was determined by the Ossila software. To account for changes in roughness between the copolymer films, the contact angle of the rough surface (θ_w) was calculated using the Wenzel equation: $\cos\theta_w = r\cos\theta_e$ where r is the roughness factor, defined as the ratio of the actual area divided by the projected area, with both areas calculated from the AFM images.

2.3.3. Atomic Force Microscopy. The surface morphology of the electropolymerized films was imaged using AFM (NanoWizard II; JPK Instruments AG Berlin, Germany) via an intermittent contact mode. Images of 50 × 50 μm regions were captured using silicon cantilevers at a scan rate of 0.5 Hz with a nominal spring constant of

https://doi.org/10.1021/acsami.4c03229
ACS Appl. Mater. Interfaces XXXX, XXX, XXX−XXX

32 N/m and a resonant frequency of 367 kHz (Type ACT, AppNano, Mountain View, CA, USA). The images were captured at a resolution of 512 × 512 pixels, where each pixel represented a height profile measurement. Post-analysis was performed using JPK data processing software. A total of 262,144 data points were collected from each of the co-PEDOT samples and analyzed to generate the Gaussian distributions, which depicted the range of height profiles within each sample. The random and Gaussian height profiles provided insights into the surface morphology of the co-PEDOT films, enabling visualization and characterization of their topographical features.

2.4. Optical, Electrochemical, and OECT Characterization. *2.4.1. In Situ Spectroelectrochemistry.* This method was performed to probe the optoelectronic properties of the copolymers synthesized on the ITO substrates using a UV−vis−NIR spectrometer (Lambda 1050, PerkinElmer) with wavelengths ranging from 350 to 900 nm. First, the optical absorbance of each copolymer film was recorded immediately after synthesis. The copolymer films (used as working electrodes) were then positioned in a cuvette filled with 0.1 M NaCl aqueous electrolyte and containing a saturated Ag/AgCl reference electrode and a platinum wire as the counter electrode. The three-electrode setup was connected to an Ivium potentiostat used to apply potentials ranging from −0.4 to +0.8 V in incremental steps of +0.1 V. The applied voltage was held for 30 s, and then the absorption spectra were recorded while maintaining the films under the applied potential.

2.4.2. Cyclic Voltammetry. The electroactivity of the copolymer films was characterized by performing CV ranging from −0.4 to +0.8 V in 0.1 M NaCl electrolyte using an Ivium potentiostat with the three-electrode system.

2.4.3. Electrochemical Impedance Spectrometry. EIS was performed to investigate ion diffusion in the polymer films as a function of frequency and applied potential. The EIS was recorded using a three-electrode setup linked to an Ivium potentiostat. The measurements were performed at two potentials, −0.4 and +0.4 V, between 10^{-1} and 10^{5} Hz with an AC potential of 10 mV. The value of the capacitance was noted at 10^{-1} Hz and normalized by the dimensions of the film (width, length, and thickness) to obtain the volumetric capacitance (C^*). The thickness (d) was measured for dry films by using a 3D Keyence Laser Microscope. A scratch was made in the middle of the film. After leveling, the height difference between the film and the substrate across the scratch was measured to obtain the film thickness, calculated by taking the average value of 3 different measured areas.

2.4.4. Current−Voltage (I−V) Curves. The $I-V$ curves of dry copolymer films synthesized on single-channel devices were recorded using a Keithley 2401 source-measure unit by sweeping the potential between −0.4 and +0.4 V and measuring the current. The resistance R was then determined from the slope of V versus I according to Ohm's law. The conductivity σ was calculated according to the following equation: $\sigma = \frac{L}{Rwd}$.

2.4.5. OECT Characterization. Transfer and output curves of copolymer films grown on IDME substrates were recorded in 0.1 M NaCl solution using a saturated Ag/AgCl reference electrode as the gate electrode and a pair of Keithley 2401 source-measure units. Maximum transconductance g_{max}, threshold voltage V_{Th}, I_{ON}/I_{OFF} ratio, and μC^*, where μ is the charge carrier mobility, were extracted from the transfer curves following the literature and briefly outlined in the Supporting Information.[42]

2.5. Post-functionalization. Copolymer films on ITO, co-PEDOT-1, -2, -3, -4, and -5, were immersed in 1 mL of 0.1 M MES buffer solution (pH = 6.5) containing 0.1 M EDC and 0.2 M NHS for 1 h to activate the carboxylic groups. Films were then transferred to a vial containing 1 mL of 0.1 M APMA prepared in sodium hydrogen carbonate solution pH = 8.5 for 1 h. Copolymer films serving as controls were soaked in MES buffer without EDC and NHS for 1 h, followed by their incubation in 0.1 M APMA solution. Eliminating the activation step of the carboxylic group with NHS and EDC allows us to test for electrostatic interactions that might occur between the ionized nature side groups on the copolymers and the protonated nature of APMA. All copolymers' films were then washed by soaking in PBS (0.1 M, pH = 7.4) for 15 min, and this step was repeated three times. Subsequently, the films were air-dried overnight, and XPS was employed to characterize the nitrogen content. CV, EIS, and OECT characterization were performed on surface-functionalized co-PEDOT-2 (co-PEDOT-2f) to investigate the effect of post-functionalization on electrochemical performance.

2.6. Statistical Analysis. Data are presented as an average ± standard deviation. One-way ANOVA was used to analyze the data, with values of $p < 0.05$ considered significant.

3. RESULTS AND DISCUSSION

Stable functionalized PEDOT-based copolymers with varying contents of the ionized EDOTS (68−24%) were successfully synthesized. This was made possible by the oxygen plasma treatment that we applied here on the conductive substrates prior to electropolymerization. The surface of plasma-treated ITO has been shown to have improved polarity due to the introduction of oxygen and removal of hydrocarbon contaminants.[43] A polar surface will enhance the adhesion of the two monomers EDOTCOOH and EDOTS, facilitating the synthesis of copolymers with variable composition. This resulted in the development of OMIECs with demonstrated efficient ion/electron transport and versatility of post-functionalization.

3.1. Electropolymerization of Copolymer Films. We successfully synthesized OMIEC copolymers with tunable chemical compositions by potentiodynamic electropolymerization of the two monomers, EDOTS and EDOTCOOH, in different molar ratios (Figure 1 and Table S1).

We observed during polymerization an increase in the current as the number of scanning cycles increased, indicating that a polymer was growing on the plasma-treated ITO substrate (Figure S1A−E). This was also confirmed by visual inspection, whereby a continuous dark blue film could be seen on the working electrodes for all feed ratios. The E_{onset} of the polymerization shows a decrease in value with the decreasing proportion of EDOTS, varying from 0.97 ± 0.01 V for co-PEDOT-1 to 0.93 ± 0.02 V for co-PEDOT-5 (Figure S1F). We have previously shown that EDOTCOOH has an improved interfacial contact with the ITO electrode due to the adsorption of the carboxylic groups to its surface.[38] This in turn leads to a lower E_{onset} for the copolymers with higher ratios of EDOTCOOH.[44] Furthermore, all synthesized copolymers remained stable and adhered on the substrate during characterization, in contrast to our previous protocol that used nontreated conductive substrates limiting the synthesis of stable copolymers with no more than 45% EDOTS.[38]

3.2. Structural and Surface Morphology Characterization. We used XPS to determine the ratio of the sulfonic to carboxylic acid groups in each copolymer formulation. Analysis of the S 2p spectra of all five copolymers (Figure S2 and Table S2) revealed peaks related to the sulfur in the thiophene ring that we have assigned as a neutral sulfur [163.9 eV (S $2p_{3/2}$) and 165.0 eV (S $2p_{1/2}$)] and an electron-deficient sulfur [165.3 eV (S $2p_{3/2}$) and 166.5 eV (S $2p_{1/2}$)].[45] The electron-deficient sulfur indicates that the copolymers are partially doped, despite the fact that the films were subjected to −0.4 V at the end of the potentiodynamic electrosynthesis. We attribute this to self-acid-doping introduced by the EDOTS monomer bearing a sulfonic acid group.[46] However, oxygen doping of electropolymerized PEDOT:Cl reduced at −0.5 and −0.9 V has been demonstrated upon exposure to air,[47] with the authors speculating that electron transfer occurs from the reduced

https://doi.org/10.1021/acsami.4c03229
ACS Appl. Mater. Interfaces XXXX, XXX, XXX−XXX

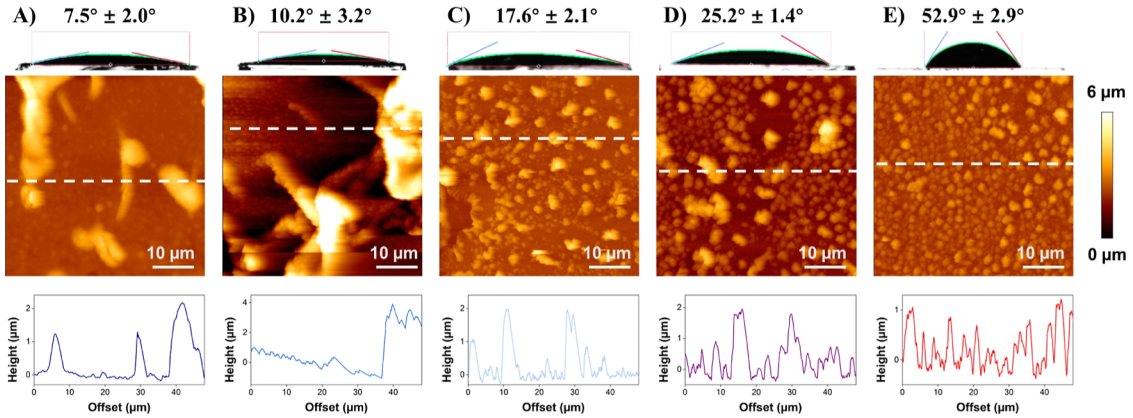

Figure 2. Contact angle θ_e measured by the contact angle goniometer (top half) and AFM micrographs and height profiles (bottom half) of (A) co-PEDOT-1, (B) co-PEDOT-2, (C) co-PEDOT-3, (D) co-PEDOT-4, and (E) co-PEDOT-5. Scale bar: 10 μm. The white dash lines correspond to the area over which the height profiles were measured.

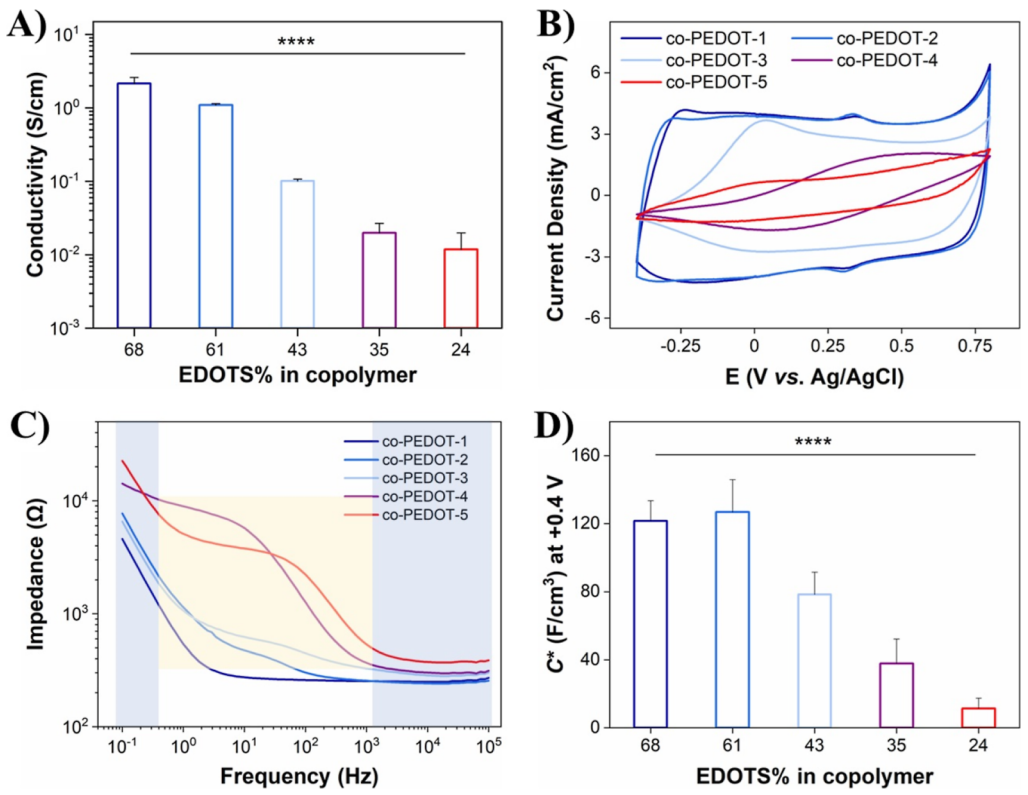

Figure 3. (A) Conductivity of dry copolymer films presented on a log scale ($p < 0.0001$). (B) Cyclic voltammograms of the copolymer films under a scan rate of 50 mV/s versus a saturated Ag/AgCl reference electrode in 0.1 M NaCl solution. (C) Impedance magnitude versus frequency plots under +0.4 V voltage versus a saturated Ag/AgCl electrode in 0.1 M NaCl solution. (D) Volumetric capacitance (C^*) extracted from the Bode plots at +0.4 V and 0.1 Hz ($p < 0.0001$).

PEDOT to oxygen, forming intermediate superoxide counterions. Considering that our copolymer films were at −0.4 V at the end of the synthesis, oxygen doping could not be ruled out. A small peak of low intensity (<3.5%) appeared at 168.05 (S $2p_{3/2}$) and 169.25 eV (S $2p_{1/2}$), which we assign to a sulfone that might have resulted from overoxidation of the films during the electropolymerization procedure.[48,49] The sulfonic groups of EDOTS were observed at 168.35 eV (S $2p_{3/2}$) and 169.55 eV (S $2p_{1/2}$) in all five copolymers (Figure S2). Our quantitative analysis of the sulfur environment reveals that the % of EDOTS in the copolymers decreases from 68.2% for co-PEDOT-1 to 24.1% for co-PEDOT-5 in accordance with the monomer feed ratio (Figure 1C). The XPS data confirms that we can successfully synthesize PEDOT-based copolymers with tailored chemical composition by simply varying the ratio of EDOTS to EDOTCOOH monomer.

As would be expected, varying the ratio of the sulfonic to carboxylic groups in the copolymer films had an impact on their hydrophilicity, as revealed by the contact angle (Figure 2). The measurements were conducted on films immediately after synthesis, which were partially oxidized, as shown in their UV−vis spectra (Figure S4). The contact angle θ_w calculated according to the Wenzel model (Figure 2 and Table S3) was the lowest for co-PEDOT-1, indicating the very hydrophilic

https://doi.org/10.1021/acsami.4c03229
ACS Appl. Mater. Interfaces XXXX, XXX, XXX−XXX

nature of the copolymer containing significant % of sulfonic acid groups. As the sulfonic-modified monomer ratio was decreased, the hydrophilicity of the films decreased, with co-PEDOT-5 exhibiting the highest contact angle.

We then characterized the copolymer films using AFM to probe the effect of varying the chemical composition on the films' morphology (Figure 2). The 2D micrographs reveal a drastic change in the morphology between the copolymers. co-PEDOT-1 and -2 had a smooth homogeneous surface marked with few localized areas of elevated heights (~2 μm) and significant width (~8 μm) (Figure 2A,B). As the ratio of EDOTS decreased in the copolymer, these areas became smaller but more numerous (Figure 2C−E). This trend is in line with the height histograms of the whole sample area (50 × 50 μm^2), where co-PEDOT-3, -4, and -5 films have smaller features than co-PEDOT-1 and -2 (Figure S3). We attribute these changes in morphology to the EDOTCOOH portion of the copolymer. We know from our previous study that EDOTCOOH adheres better than EDOTS to the working electrode, as was shown by a prewave in its first voltammogram during the synthesis.[38] In co-PEDOT-1 and -2 that have higher amounts of EDOTS than EDOTCOOH, adhesion of EDOTCOOH might have been limited to confined areas of the electrode surface, resulting in its localized nucleation and growth, which appear as few wide and bright spots. As the ratio of EDOTCOOH was significantly increased in the feed ratio, a more uniform adhesion of the monomer was expected to occur on the electrode surface, thereby resulting in a more homogeneous growth, accounting for the less wide but more dense bright spots in the micrographs (Figure 2C−E). It might be inferred from these micrographs that the electrosynthesis of co-PEDOT-1 and -2 might have resulted in a "block copolymer", but as the EDOTCOOH ratio is increased, a random copolymer is formed.

3.3. Optical and Electrochemical Properties. We recorded the electronic spectra of the electropolymerized films following the synthesis. All copolymers were in a doped state, as indicated by the increased absorption in the region extending above 600 nm (dash lines in Figure S4), indicative of polaron formation in the polymers. These peaks confirm that the copolymers are partially doped, likely caused by oxygen doping and self-acid-doping imparted by the sulfonic acid side groups.[46,47]

The electropolymerized copolymers exhibited a conductive nature without adding any external dopants (Figure 3A). The conductivities of co-PEDOT-1, and -2 were 2.14 ± 0.45 and 1.10 ± 0.05 S/cm, respectively. These values are comparable to other sulfonated PEDOT analogues.[39,50,51] As the sulfonic acid ratio decreased in co-PEDOT-3, -4, and -5, we note a significant decrease in the films' conductivity (Figure 3A). However, the conductivity of co-PEDOT-4 ($1.99 \times 10^{-2} \pm 0.01 \times 10^{-2}$ S/cm) was an order of magnitude higher than our previously published PEDOT copolymer with similar composition and ratios of EDOTS and EDOTCOOH but electropolymerized on untreated plasma ITO substrates.[38] This significant improvement in conductivity can be attributed to the plasma treatment of the surface prior to electropolymerization. The doped nature of the copolymer films observed in the UV−vis spectra and the conductivity measurements agree with the XPS data that revealed the presence of an electron deficient sulfur (Figure S2).

We then tested whether the copolymers could switch between oxidation states in response to the applied potentials (Figure S4). Subject to −0.4 V, we observe a new absorption peak at ~550 nm that corresponds to $\pi-\pi^*$ transitions, indicating that the copolymers are converting to a neutral state. However, absorption remains high at wavelengths >700 nm, confirming that the copolymers are only partially reduced at this voltage. Incremental increases of the applied voltages from −0.3 to +0.8 V revert the neutral fraction of the copolymers to an oxidized state, as demonstrated by the gradual decrease of the $\pi-\pi^*$ transition peak and the increase in the absorption >600 nm corresponding to polaron formation (Figure S4). Their electroactivity in aqueous electrolytes was further shown by CV (Figure 3B). Copolymers with higher ratios of sulfonic acid groups (co-PEDOT-1, -2, and -3) exhibit higher current density and capacitance in comparison to copolymers with increased ratios of carboxylic groups (co-PEDOT-4 and -5).

We then performed EIS measurements to further probe the extent of ion penetration and changes in the copolymers' oxidation states when subjected to applied potentials in aqueous electrolytes. Switching the potential from −0.4 to +0.4 V results in a significant decrease in the impedance of all copolymer films in the low frequency regime (<10 Hz, Figure S5). This indicates that charge carriers are formed at +0.4 V, which in turn results in the diffusion of counterions inside the film. Comparing the impedance spectra of the copolymers at +0.4 V reveals that varying the ratio of the sulfonic acid to the carboxylic acid groups alters the electric characteristics of the copolymers (Figure 3C). The impedance spectrum of co-PEDOT-1 shows a resistive behavior in the mid-to-high frequency range (10−10^5 Hz) and a capacitive behavior in the low frequency range (<100 Hz), typical of PEDOT coated electrodes.[52,53] However, we identified three regions in the impedance spectra as the ratio of carboxylic groups increased in the copolymer: Region I—high frequency (>10^3 Hz)—resistive region, Region II—mid frequency range (1−10^3 Hz), and Region III—low frequency (<1 Hz)—capacitive region. No significant change in impedance is observed in regions I and III, with all five copolymers exhibiting a frequency-independent resistive behavior in Region I or a frequency-dependent capacitive behavior in Region III.[52] The impedance spectra vary mostly between the copolymers in Region II, i.e., $f \sim 1$ to 10^3 Hz. We observe impedance and phase features (Figure S5) typical of those observed in the assessment of barrier models where the ion movement is impeded.[54,55] The impedance gradually increases in this region, with the increase being more pronounced as the ratio of carboxylic groups in the copolymers varied from 32 to 76%. We also observe a plateau region becoming very apparent for co-PEDOT-4 and -5, indicating a more significant impediment to the ion flux in these materials. We extracted and calculated from the EIS data the volumetric capacitance C^* of the copolymers at +0.4 V as a function of its sulfonic group content (Figure 3D and Table S4). C^* decreases significantly from 121 ± 12 F/cm^3 for co-PEDOT-1 (containing 68% sulfonic acid groups) to 11 ± 6 F/cm^3 for co-PEDOT-5 (containing 24% sulfonic acid groups). Of note, the C^* values of co-PEDOT-1 and -2 are significantly higher than other reported conjugated polyelectrolyte copolymers such as those based on sulfonic-modified thiophene copolymerized with 3-hexylthiophene, in which the sulfonate group was counterbalanced with ammonium cation to enable the chemical synthesis of the copolymer.[15] However, decreasing the content of the sulfonic groups to lower than 50% impacted the ion transport capability of the copolymer films as revealed by the significantly decreased

https://doi.org/10.1021/acsami.4c03229
ACS Appl. Mater. Interfaces XXXX, XXX, XXX−XXX

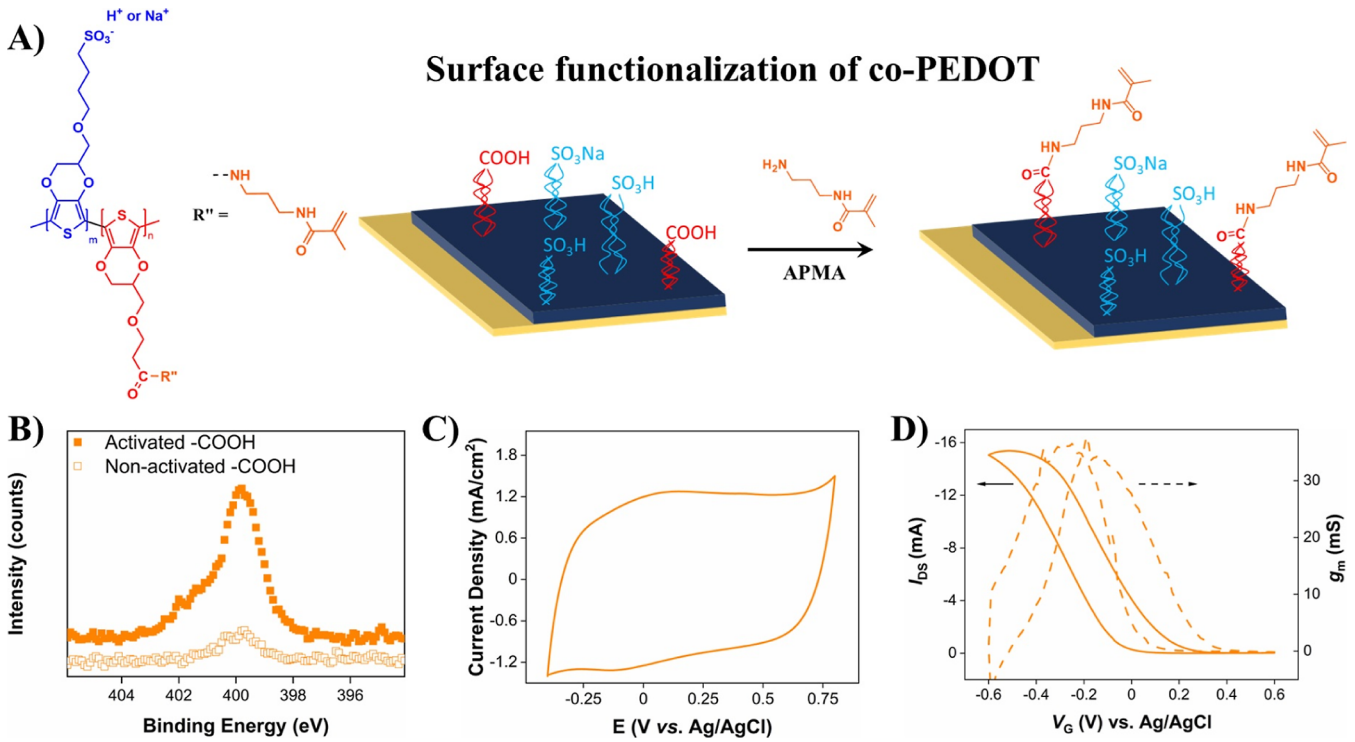

Figure 4. (A) Chemical structure of the copolymer post-functionalized with APMA and a schematic presentation of surface functionalization. (B) XPS N 1s spectra of co-PEDOT-2f treated with APMA, with or without the activation of the carboxylic groups. (C) Cyclic voltammogram of co-PEDOT-2f under a scan rate of 50 mV/s versus a saturated Ag/AgCl electrode in 0.1 M NaCl solution. (D) Transfer (solid line) and transconductance (dash line) curves of co-PEDOT-2f measured at $V_D = -0.6$ V in 0.1 M NaCl solution and using a saturated Ag/AgCl as the gate electrode.

values of the C^* (Figure 3D) (one-way ANOVA, $p < 0.0001$). This is likely due to the electron transport being less efficient in these copolymers, as revealed by their decreased conductivity values (Figure 3A), which in turn will imply less available charge carriers to attract counterions in the films. Furthermore, the morphology of conjugated polymer films influences ion diffusion within the bulk.[42,56,57] Our AFM images revealed significant differences in the films' morphology as a function of the EDOTS content, which might also explain why ionic transport varied between the copolymers.

3.4. OECT Properties. The conductivity of the copolymer films and their evident electrochemical performance in an aqueous electrolyte support their utility as bioelectrodes or organic conductors in bioapplications. Similarly, their noticeable volumetric capacitances point toward their potential application as active channel materials in OECT devices. To this end, we evaluated their device performance by directly electropolymerizing copolymers on commercial IDMEs. Our synthetic protocols resulted in copolymer films that bridged all of the electrodes of the IDME. Figure S6 presents illustrative examples of the transfer and transconductance curves of each copolymer. Output curves and device parameters extracted from these data are presented in Figure S7 and Table S4, respectively. All five copolymer films exhibited transistor characteristics, as would be expected from their hydrophilic nature revealed by the contact angle measurements (Figure 2 and Table S3) and their volumetric capacitances that confirm efficient mixed ion-electron transport (Figure 3D). The OECT devices were not fully OFF at zero voltage, indicating that the devices operate in hybrid accumulation-depletion mode. The copolymers displayed good signal-to-noise ratio as demonstrated by the high I_{ON}/I_{OFF} ratio measured for all copolymers. Furthermore, I_{ON}/I_{OFF} significantly varied with the content of the sulfonic groups (one-way ANOVA, $p = 0.0002$). Similarly, the maximum transconductance normalized by the film thickness $g_{max,norm}$ revealed a decreasing trend between the copolymers as the ratio of ionized sulfonate groups decreased in their chemical composition (one-way ANOVA, $p = 0.0138$). We calculated the charge carrier mobility μ from the plot of $\sqrt{I_D}$ versus V_G (details in the Supporting Information, Table S4). We observed an increasing trend in mobility as the sulfonic groups in the copolymers decreased (one-way ANOVA, $p = 0.0464$). As we inferred from the AFM micrographs, co-PEDOT-1 and -2 likely have a "blocky" architecture, which, in turn, will influence the backbone mobility. On the other hand, co-PEDOT-3, -4, and -5 had a more homogeneous surface topography that we attribute to the formation of a random copolymer, whereby the mobility might have been improved as a result.

Device characteristics are highly dependent on the channel width and length, single- or multielectrode devices, and the thickness of the channel material. In a recent review article, for instance, Inal and coauthors[42] highlighted the importance of accurate measurement of the thickness, accounting for the type of conductive substrates the channel material is deposited on. Furthermore, there is variation in how device parameters are reported such as how V_{Th} is determined or g_{max} normalized. Additionally, consideration should be made to the polymerization process used to synthesize the active channel material; for instance, electrochemical properties vary between a PEDOT backbone produced by chemical or electropolymerization.[58] When examining PEDOT-based OECTs in which the

https://doi.org/10.1021/acsami.4c03229
ACS Appl. Mater. Interfaces XXXX, XXX, XXX−XXX

PEDOT channel was prepared by electropolymerization, reported volumetric capacitances range from 150 to 226 F/cm^3,[4,59] mobilities from 10^{-5} to 1 cm^2/V.s,[60,61] I_{ON}/I_{OFF} from 180 to >10,000,[62,63] and V_{Th} from 0.2 to 0.79 V.[4,61] While broadly our OECT characteristics are within these ranges, a comprehensive comparison to other published OECT devices is challenging and has limited reliability. We therefore focused our discussion on comparing the copolymers within our study having the same device geometry and consistent measurement techniques. Our device characterizations confirm that the copolymers can serve effectively as tunable *p*-type channel materials with noticeable amplification performance. Of note, our copolymers served as channel materials in their ionized form, in contrast to the many other sulfonic-modified conjugated polymers that require capping with ammonium cations prior to OECT testing to prevent their dissolution in aqueous electrolytes.[10,11,14,15,39,64−66]

3.5. Post-functionalization and Electrochemical Properties. Our synthetic design of the copolymers as OMIECs was driven by the introduction of not only ionically conductive entities but also chemical handles that provide post-functionalization capabilities of the synthesized polymers. We used APMA that has an amine group as a model chemical compound to react with the carboxylic groups activated with EDC and NHS in the copolymers (Figure 4A).

We also soaked the copolymers in a solution of APMA without activation of the carboxylic groups to test for ionic interactions. Qualitative analysis of the XPS survey scan reveals the presence of the element nitrogen in all copolymers. Figures 4B and S8 show the N 1s spectra before and after activation of the carboxylic group. We observe that all copolymers contained nitrogen after treatment with APMA; however, samples in which the carboxylic groups were activated using EDC/NHS exhibit higher intensities, suggesting successful chemical functionalization of our copolymers. We attribute the presence of nitrogen in copolymers without activation to electrostatic interactions between the positively charged APMA and the negatively charged sulfonic and carboxylic groups. The pH of the reaction was 8.5, at which both the sulfonate and carboxylic groups were ionized. Similarly, based on the reported pK_a value of APMA (~9),[67] the amine groups will be protonated, enabling the ionic interactions observed.

Among the 5 copolymers characterized in this study, co-PEDOT-2 exhibited optimal electrochemical performance in terms of its electroactivity, volumetric capacitance, and normalized transconductance. Consequently, we chose to characterize the electrochemical performance of co-PEDOT-2 modified with APMA, co-PEDOT-2f, to establish that surface functionalization does not impede its role as an OMIEC. CV (Figure 4C) and electrochemical impedance spectroscopy (Figure S9) confirmed that the copolymer retains its electroactivity post-functionalization. Similarly, the performance of co-PEDOT-2f as a channel material was not affected by the functionalization; the output drain current and the transconductance of co-PEDOT-2f were of comparable values to those of co-PEDOT-2 (Figure 4D and Table S4). This confirms that our design strategy of a copolymer that combines both ionic/electronic conductivity with post-functionalization is a viable approach to develop OMIECs with tailored properties.

4. CONCLUSIONS

We presented a synthetic strategy for the development of OMIECs that enabled ion−electron conduction with post-functionalization. By oxygen plasma treatment of the conductive substrates, we were successful in synthesizing a novel series of functional PEDOT-based copolymers, using different feed ratios of EDOTS and EDOTCOOH. This was not previously possible with untreated substrates, which limited the synthesis of stable copolymers with no more than 45% EDOTS in their composition. We utilized electropolymerization in an aqueous electrolyte, demonstrating that the copolymers can be obtained using a time-efficient synthetic technique with ease of fabrication immediately on the targeted substrate. Of significance is the physical stability of the copolymers in water-based media, despite the high content of the ionized EDOTS, for example, in co-PEDOT-1 and -2. This in turn resulted in tuning of the copolymers' conductivities, attributed to self-acid-doping provided by the sulfonic groups. Additionally, plasma treatment of the substrate appears to enhance the conductivity of the copolymer having a similar composition to our previously reported copolymer on untreated substrates. This is likely due to changes in polymer chain packing that require dedicated studies to confirm. The improved conductivity is key for their bioapplications, such as passive electrodes or active OECT devices, highlighting a versatile utility of the copolymers. Our characterization included morphology studies as well as an in-depth analysis of all electrochemical properties, enabling us to show the tunability of the copolymers' properties; future studies should focus on investigating the electronic stability of copolymer-based bioelectrodes or OECT devices in response to continuous or intermittent cycling to probe their longevity. Additionally, our synthetic design not only enabled efficient ion/electron transport but also offered the versatility of post-functionalization without impacting electrochemical performance. Designing conjugated copolymers, as opposed to homopolymers, facilitates the development of materials with more than one functionality, which is critical to tailor the properties of the OMIECs so they meet specific requirements of the many bioelectronic applications.

■ ASSOCIATED CONTENT

Supporting Information

The Supporting Information is available free of charge at https://pubs.acs.org/doi/10.1021/acsami.4c03229.

Details of the formulations used for the synthesis of the copolymers; XPS fitting parameters for S 2p; CV of the electropolymerization of different ratios of EDOTS and EDOTCOOH and E_{onset} of each feed ratio estimated from the first anodic voltammogram; XPS S 2p analysis; AFM Gaussian height profiles; in situ spectroelectrochemistry; Bode and phase angle plots; transfer, transconductance, and output curves; OECT device parameters and a description of their calculation; XPS N 1s analysis of post-functionalization; and Bode and phase angle plots of the post-functionalized co-PEDOT-2f (PDF)

■ AUTHOR INFORMATION

Corresponding Author

Damia Mawad − *School of Materials Science and Engineering, UNSW Sydney, Sydney, New South Wales 2052, Australia;*

https://doi.org/10.1021/acsami.4c03229
ACS Appl. Mater. Interfaces XXXX, XXX, XXX−XXX

orcid.org/0000-0002-6965-3232;
Email: damia.mawad@unsw.edu.au

Authors

Jiaxin Wu − *School of Materials Science and Engineering, UNSW Sydney, Sydney, New South Wales 2052, Australia*
Modi Gu − *School of Materials Science and Engineering, UNSW Sydney, Sydney, New South Wales 2052, Australia*
Lorenzo Travaglini − *School of Materials Science and Engineering, UNSW Sydney, Sydney, New South Wales 2052, Australia; School of Biotechnology and Biomolecular Sciences, UNSW Sydney, Sydney, New South Wales 2052, Australia*
Antonio Lauto − *School of Science, Western Sydney University, Penrith, New South Wales 2751, Australia;* orcid.org/0000-0003-4593-5603
Daniel Ta − *School of Science, Western Sydney University, Penrith, New South Wales 2751, Australia*
Pawel Wagner − *Intelligent Polymer Research Institute and ARC Centre of Excellence for Electromaterials Science, University of Wollongong, Wollongong, New South Wales 2522, Australia;* orcid.org/0000-0003-1926-9862
Klaudia Wagner − *Intelligent Polymer Research Institute and ARC Centre of Excellence for Electromaterials Science, University of Wollongong, Wollongong, New South Wales 2522, Australia;* orcid.org/0000-0001-6803-4221
Erica Zeglio − *Wallenberg Initiative Materials Science for Sustainability, Department of Materials and Environmental Chemistry, Stockholm University, 114 18 Stockholm, Sweden; AIMES − Center for the Advancement of Integrated Medical and Engineering Sciences, Department of Neuroscience, Karolinska Institute, 17177 Stockholm, Sweden; Digital Futures, Stockholm SE-100 44, Sweden*
Achilleas Savva − *Bioelectronics Section, Department of Microelectronics, Faculty of Electrical Engineering, Mathematics and Computer Science, Delft University of Technology, Delft 2628 CD, The Netherlands*
David Officer − *Intelligent Polymer Research Institute and ARC Centre of Excellence for Electromaterials Science, University of Wollongong, Wollongong, New South Wales 2522, Australia;* orcid.org/0000-0001-5465-9781

Complete contact information is available at: https://pubs.acs.org/10.1021/acsami.4c03229

Author Contributions

J.W and M.G. contributed equally. J.W and M.G carried out laboratory research including synthesis and characterization of the copolymer films, performed data analysis, and prepared draft manuscript. A.L. and D.T. performed the AFM characterization and analysis. D.M., P.W, and D.O. conceived and designed the study. All authors contributed to the preparation of the manuscript and have given approval to the final version of the manuscript.

Funding

D.M., D.O., and A.L. acknowledge the Australian Research Council, Discovery Project Grant DP190102560, Australia, for funding this research.

Notes

The authors declare no competing financial interest.

■ ACKNOWLEDGMENTS

The authors would like to acknowledge the use of facilities and the assistance of Dr. Bill Bin Gong in the Solid State and Elemental Analysis Unit under the Mark Wainwright Analytical Centre at UNSW Sydney.

■ ABBREVIATIONS

AFM, atomic force microscopy; APMA, *N*-(3-aminopropyl)-2-methylacrylamide hydrochloride; BE, binding energy; C^*, volumetric capacitance; CV, cyclic voltammetry; *d*, thickness; EDC, 1-ethyl-3-(3-(dimethylamino)propyl)carbodiimide; EDOTCOOH, 3-[(2,3-dihydrothieno[3,4-*b*][1,4] dioxin-2-yl)methoxy] propanoic acid; EDOTS, sodium 4-[(2,3-dihydrothieno[3,4-*b*][1,4]dioxin-2-yl)methoxy]butane-1-sulfonate; EIS, electrochemical impedance spectrometry; E_{onset}, onset potential of the monomer; HCl, hydrochloric acid; H_2O_2, hydrogen peroxide; IDME, interdigitated microelectrode; ITO, indium tin oxide; *I*−*V*, current−voltage; *L*, length; $LiClO_4$, lithium perchlorate; MES buffer, 2-(*N*-morpholino)-ethanesulfonic acid; NaCl, sodium chloride; $NaHCO_3$, sodium hydrogen carbonate; NaOH, sodium hydroxide; NH_4OH, ammonium hydroxide; NHS, *N*-hydroxysuccinimide; OECT, organic electrochemical transistor; OMIECs, organic mixed ionic−electronic conductors; PBS, phosphate-buffered saline; PEDOT, poly(3,4-ethylenedioxythiophene); PEDOT:PSS, poly(3,4-ethylenedioxythiophene):poly(styrenesulfonate); PEO, poly(ethylene oxide); P3HT, poly(3-hexylthiophene); *w*, width; XPS, X-ray photoelectron spectroscopy

■ REFERENCES

(1) Lu, Z.; Pavia, A.; Savva, A.; Kergoat, L.; Owens, R. M. Organic Microelectrode Arrays for Bioelectronic Applications. *Mater. Sci. Eng., R* **2023**, *153*, 100726.
(2) Marks, A.; Griggs, S.; Gasparini, N.; Moser, M. Organic Electrochemical Transistors: An Emerging Technology for Biosensing. *Adv. Mater. Interfaces* **2022**, *9* (6), 2102039.
(3) Tropp, J.; Meli, D.; Rivnay, J. Organic Mixed Conductors for Electrochemical Transistors. *Matter* **2023**, *6* (10), 3132−3164.
(4) Fenoy, G. E.; Hasler, R.; Quartinello, F.; Marmisollé, W. A.; Lorenz, C.; Azzaroni, O.; Bäuerle, P.; Knoll, W. Clickable" Organic Electrochemical Transistors. *JACS Au* **2022**, *2* (12), 2778−2790.
(5) Paulsen, B. D.; Tybrandt, K.; Stavrinidou, E.; Rivnay, J. Organic Mixed Ionic-Electronic Conductors. *Nat. Mater.* **2020**, *19* (1), 13−26.
(6) Frankenstein, H.; Stein, E.; Stolov, M.; Koifman Khristosov, M.; Freger, V.; Frey, G. L. Blends of Polymer Semiconductor and Polymer Electrolyte for Mixed Ionic and Electronic Conductivity. *J. Mater. Chem. C* **2021**, *9* (24), 7765−7777.
(7) Zhu, Z.; Zhang, L.; Smith, S.; Fong, H.; Sun, Y.; Gosztola, D. Fluorescence Studies of Electrospun MEH-PPV/PEO Nanofibers. *Synth. Met.* **2009**, *159* (14), 1454−1459.
(8) Menezes, N. P.; Nicolini, T.; Barker, M.; Mariano, A. A.; Dartora, C. A.; Wantz, G.; Stingelin, N.; Abbas, M.; Dautel, O. J.; Thuau, D.; Thuau, D. Improved Stability of Organic Electrochemical Transistor Performance with a Low Swelling Mixed Conducting Polymer: A Comparative Study with PEDOT:PSS. *J. Mater. Chem. C* **2023**, *11* (19), 6296.
(9) Erothu, H.; Kolomanska, J.; Johnston, P.; Schumann, S.; Deribew, D.; Toolan, D. T. W.; Gregori, A.; Dagron-Lartigau, C.; Portale, G.; Bras, W.; Arnold, T.; Distler, A.; Hiorns, R. C.; Mokarian-Tabari, P.; Collins, T. W.; Howse, J. R.; Topham, P. D. Synthesis, Thermal Processing, and Thin Film Morphology of Poly(3-Hexylthiophene)-Poly(Styrenesulfonate) Block Copolymers. *Macromolecules* **2015**, *48* (7), 2107−2117.
(10) Zeglio, E.; Eriksson, J.; Gabrielsson, R.; Solin, N.; Inganäs, O. Highly Stable Conjugated Polyelectrolytes for Water-Based Hybrid Mode Electrochemical Transistors. *Adv. Mater.* **2017**, *29* (19), 1605787.
(11) Zeglio, E.; Vagin, M.; Musumeci, C.; Ajjan, F. N.; Gabrielsson, R.; Trinh, X. T.; Son, N. T.; Maziz, A.; Solin, N.; Inganäs, O.

Conjugated Polyelectrolyte Blends for Electrochromic and Electrochemical Transistor Devices. *Chem. Mater.* **2015**, *27* (18), 6385−6393.
(12) Moser, M.; Wang, Y.; Hidalgo, T. C.; Liao, H.; Yu, Y.; Chen, J.; Duan, J.; Moruzzi, F.; Griggs, S.; Marks, A.; Gasparini, N.; Wadsworth, A.; Inal, S.; McCulloch, I.; Yue, W. Propylene and Butylene Glycol: New Alternatives to Ethylene Glycol in Conjugated Polymers for Bioelectronic Applications. *Mater. Horiz.* **2022**, *9* (3), 973−980.
(13) Tropp, J.; Meli, D.; Wu, R.; Xu, B.; Hunt, S. B.; Azoulay, J. D.; Paulsen, B. D.; Rivnay, J. Revealing the Impact of Molecular Weight on Mixed Conduction in Glycolated Polythiophenes through Electrolyte Choice. *ACS Mater. Lett.* **2023**, *5* (5), 1367−1375.
(14) Inal, S.; Rivnay, J.; Leleux, P.; Ferro, M.; Ramuz, M.; Brendel, J. C.; Schmidt, M. M.; Thelakkat, M.; Malliaras, G. G. A High Transconductance Accumulation Mode Electrochemical Transistor. *Adv. Mater.* **2014**, *26* (44), 7450−7455.
(15) Schmode, P.; Ohayon, D.; Reichstein, P. M.; Savva, A.; Inal, S.; Thelakkat, M. High-Performance Organic Electrochemical Transistors Based on Conjugated Polyelectrolyte Copolymers. *Chem. Mater.* **2019**, *31* (14), 5286−5295.
(16) Stéphan, O.; Schottland, P.; Le Gall, P. Y.; Chevrot, C.; Mariet, C.; Carrier, M. Electrochemical Behaviour of 3,4-Ethylenedioxythiophene Functionalized by a Sulphonate Group. Application to the Preparation of Poly(3,4-Ethylenedioxythiophene) Having Permanent Cation-Exchange Properties. *J. Electroanal. Chem.* **1998**, *443* (2), 217−226.
(17) Beaumont, C.; Turgeon, J.; Idir, M.; Neusser, D.; Lapointe, R.; Caron, S.; Dupont, W.; D'Astous, D.; Shamsuddin, S.; Hamza, S.; Landry, É.; Ludwigs, S.; Leclerc, M. Water-Processable Self-Doped Conducting Polymers via Direct (Hetero)Arylation Polymerization. *Macromolecules* **2021**, *54* (12), 5464−5472.
(18) Tu, S.; Tian, T.; Vagias, A.; Huber, L. F.; Liu, L.; Liang, S.; Fischer, R. A.; Bernstorff, S.; Müller-Buschbaum, P. Modulation of Electronic and Ionic Conduction in Mixed Polymer Conductors via Additive Engineering: Towards Targeted Applications under Varying Humidity. *Chem. Eng. J.* **2023**, *477*, 147034.
(19) Kim, B.; Na, J.; Lim, H.; Kim, Y.; Kim, J.; Kim, E. Robust High Thermoelectric Harvesting Under a Self-Humidifying Bilayer of Metal Organic Framework and Hydrogel Layer. *Adv. Funct. Mater.* **2019**, *29* (7), 1807549.
(20) Wang, H.; Ail, U.; Gabrielsson, R.; Berggren, M.; Crispin, X. Ionic Seebeck Effect in Conducting Polymers. *Adv. Energy Mater.* **2015**, *5* (11), 1500044.
(21) Lin, C. H.; Luo, S. C. Zwitterionic Conducting Polymers: From Molecular Design, Surface Modification, and Interfacial Phenomenon to Biomedical Applications. *Langmuir* **2022**, *38* (24), 7383−7399.
(22) Biglari, N.; Zare, E. N. Conjugated Polymer-Based Composite Scaffolds for Tissue Engineering and Regenerative Medicine. *Alexandria Eng. J.* **2024**, *87*, 277−299.
(23) Jiang, X.; Shi, C.; Wang, Z.; Huang, L.; Chi, L. Healthcare Monitoring Sensors Based on Organic Transistors: Surface/Interface Strategy and Performance. *Adv. Mater.* **2024**, *36* (5), 2308952.
(24) Baker, C.; Wagner, K.; Wagner, P.; Officer, D. L.; Mawad, D. Biofunctional Conducting Polymers: Synthetic Advances, Challenges, and Perspectives towards Their Use in Implantable Bioelectronic Devices. *Adv. Phys.: X* **2021**, *6*(1)..
(25) Berezhetska, O.; Liberelle, B.; De Crescenzo, G.; Cicoira, F. A Simple Approach for Protein Covalent Grafting on Conducting Polymer Films. *J. Mater. Chem. B* **2015**, *3* (25), 5087−5094.
(26) Paquin, F.; Rivnay, J.; Salleo, A.; Stingelin, N.; Silva-Acuña, C. Multi-phase microstructures drive exciton dissociation in neat semicrystalline polymeric semiconductors. *J. Mater. Chem. C* **2015**, *3* (41), 10715−10722.
(27) Pitsalidis, C.; Pappa, A. M.; Boys, A. J.; Fu, Y.; Moysidou, C. M.; van Niekerk, D.; Saez, J.; Savva, A.; Iandolo, D.; Owens, R. M. Organic Bioelectronics for In Vitro Systems. *Chem. Rev.* **2022**, *122* (4), 4700−4790.
(28) Sitarik, P.; Nagane, S. S.; Chhatre, S.; Wu, Y.; Baugh, Q.; Martin, D. C. Synthesis and Characterization of Maleimide Functionalized Poly(3,4-Ethylenedioxythiophene) (PEDOT) Polymers. *Mater. Adv.* **2022**, *3* (14), 6037−6049.
(29) Hai, W.; Pu, S.; Wang, X.; Bao, L.; Han, N.; Duan, L.; Liu, J.; Goda, T.; Wu, W. Poly(3,4-Ethylenedioxythiophene) Bearing Pyridylboronic Acid Group for Specific Recognition of Sialic Acid. *Langmuir* **2020**, *36* (2), 546−553.
(30) Lind, J. U.; Hansen, T. S.; Daugaard, A. E.; Hvilsted, S.; Andresen, T. L.; Larsen, N. B. Solvent Composition Directing Click-Functionalization at the Surface or in the Bulk of Azide-Modified PEDOT. *Macromolecules* **2011**, *44* (3), 495−501.
(31) Zhang, S.; Xu, J.; Lu, B.; Qin, L.; Zhang, L.; Zhen, S.; Mo, D. Electrochromic Enhancement of Poly(3,4-Ethylenedioxythiophene) Films Functionalized with Hydroxymethyl and Ethylene Oxide. *J. Polym. Sci., Part A: Polym. Chem.* **2014**, *52* (14), 1989−1999.
(32) Breukers, R. D.; Gilmore, K. J.; Kita, M.; Wagner, K. K.; Higgins, M. J.; Moulton, S. E.; Clark, G. M.; Officer, D. L.; Kapsa, R. M. I.; Wallace, G. G. Creating Conductive Structures for Cell Growth: Growth and Alignment of Myogenic Cell Types on Polythiophenes. *J. Biomed. Mater. Res., Part A* **2010**, *95A* (1), 256−268.
(33) Wei, B.; Liu, J.; Ouyang, L.; Kuo, C. C.; Martin, D. C. Significant Enhancement of PEDOT Thin Film Adhesion to Inorganic Solid Substrates with EDOT-Acid. *ACS Appl. Mater. Interfaces* **2015**, *7* (28), 15388−15394.
(34) Mawad, D.; Artzy-Schnirman, A.; Tonkin, J.; Ramos, J.; Inal, S.; Mahat, M. M.; Darwish, N.; Zwi-Dantsis, L.; Malliaras, G. G.; Gooding, J. J.; Lauto, A.; Stevens, M. M. Electroconductive Hydrogel Based on Functional Poly(Ethylenedioxy Thiophene). *Chem. Mater.* **2016**, *28* (17), 6080−6088.
(35) Meng, L.; Turner, A. P. F.; Mak, W. C. Tunable 3D Nanofibrous and Bio-Functionalised PEDOT Network Explored as a Conducting Polymer-Based Biosensor. *Biosens. Bioelectron.* **2020**, *159*, 112181.
(36) Lin, T. Y.; Lo, W. Y.; Kao, T. Y.; Lin, C. H.; Wu, Y. K.; Luo, S. C. Manipulating the Distribution of Surface Charge of PEDOT toward Zwitterion-like Antifouling Properties. *Polymer* **2022**, *262*, 125507.
(37) Zhu, B.; Bryant, D. T.; Akbarinejad, A.; Travas-Sejdic, J.; Pilkington, L. I. A Novel Electrochemical Conducting Polymer Sensor for the Rapid, Selective and Sensitive Detection of Biothiols. *Polym. Chem.* **2022**, *13* (4), 508−516.
(38) Gu, M.; Travaglini, L.; Hopkins, J.; Ta, D.; Lauto, A.; Wagner, P.; Wagner, K.; Zeglio, E.; Jephcott, L.; Officer, D. L.; Mawad, D. Molecular Design of an Electropolymerized Copolymer with Carboxylic and Sulfonic Acid Functionalities. *Synth. Met.* **2022**, *285*, 117029.
(39) Tropp, J.; Mehta, A. S.; Ji, X.; Surendran, A.; Wu, R.; Schafer, E. A.; Reddy, M. M.; Patel, S. P.; Petty, A. J.; Rivnay, J. Versatile Poly(3,4-Ethylenedioxythiophene) Polyelectrolytes for Bioelectronics by Incorporation of an Activated Ester. *Chem. Mater.* **2023**, *35* (1), 41−50.
(40) Bhagwat, N.; Kiick, K. L.; Martin, D. C. Electrochemical Deposition and Characterization of Carboxylic Acid Functionalized PEDOT Copolymers. *J. Mater. Res.* **2014**, *29* (23), 2835−2844.
(41) Vaagensmith, B.; Reza, K. M.; Hasan, M. N.; Elbohy, H.; Adhikari, N.; Dubey, A.; Kantack, N.; Gaml, E.; Qiao, Q. Environmentally Friendly Plasma-Treated PEDOT:PSS as Electrodes for ITO-Free Perovskite Solar Cells. *ACS Appl. Mater. Interfaces* **2017**, *9* (41), 35861−35870.
(42) Ohayon, D.; Druet, V.; Inal, S. A Guide for the Characterization of Organic Electrochemical Transistors and Channel Materials. *Chem. Soc. Rev.* **2023**, *52* (3), 1001−1023.
(43) You, Z. Z.; Dong, J. Y. Oxygen Plasma Treatment Effects of Indium-Tin Oxide in Organic Light-Emitting Devices. *Vacuum* **2007**, *81* (7), 819−825.
(44) Paik, W. K.; Han, S.; Shin, W.; Kim, Y. Adsorption of Carboxylic Acids on Gold by Anodic Reaction. *Langmuir* **2003**, *19* (10), 4211−4216.

https://doi.org/10.1021/acsami.4c03229
ACS Appl. Mater. Interfaces XXXX, XXX, XXX−XXX

(45) Yoon, H.; Hong, J. Y.; Jang, J. Charge-Transport Behavior in Shape-Controlled Poly(3,4- Ethylenedioxythiophene) Nanomaterials: Intrinsic and Extrinsic Factors. *Small* **2007**, *3* (10), 1774−1783.
(46) Fidanovski, K.; Gu, M.; Travaglini, L.; Lauto, A.; Mawad, D. Self-Doping and Self-Acid-Doping of Conjugated Polymer Bioelectronics: The Case for Accuracy in Nomenclature. *Adv. Healthcare Mater.* **2023**, 2302354.
(47) Mitraka, E.; Jafari, M. J.; Vagin, M.; Liu, X.; Fahlman, M.; Ederth, T.; Berggren, M.; Jonsson, M. P.; Crispin, X. Oxygen-Induced Doping on Reduced PEDOT. *J. Mater. Chem. A* **2017**, *5* (9), 4404−4412.
(48) Marciniak, S.; Crispin, X.; Uvdal, K.; Trzcinski, M.; Birgerson, J.; Groenendaal, L.; Louwet, F.; Salaneck, W. R. Light Induced Damage in Poly(3,4-Ethylenedioxythiophene) and Its Derivatives Studied by Photoelectron Spectroscopy. *Synth. Met.* **2004**, *141* (1−2), 67−73.
(49) Lindberg, B. J.; Hamrin, K.; Johansson, G.; Gelius, U.; Fahlman, A.; Nordling, C.; Siegbahn, K. Molecular Spectroscopy by Means of ESCA II. Sulfur Compounds. Correlation of Electron Binding Energy with Structure. *Phys. Scr.* **1970**, *1* (5−6), 286.
(50) Zotti, G.; Zecchin, S.; Schiavon, G.; Groenendaal, L. B. Electrochemical and Chemical Synthesis and Characterization of Sulfonated Poly (3,4-Ethylenedioxythiophene): A Novel Water-Soluble and Highly Conductive Conjugated Oligomer. *Macromol. Chem. Phys.* **2002**, *203* (13), 1958−1964.
(51) Mousa, A. H.; Bliman, D.; Hiram Betancourt, L.; Hellman, K.; Ekström, P.; Savvakis, M.; Strakosas, X.; Marko-Varga, G.; Berggren, M.; Hjort, M.; Ek, F.; Olsson, R. Method Matters: Exploring Alkoxysulfonate-Functionalized Poly(3,4-Ethylenedioxythiophene) and Its Unintentional Self-Aggregating Copolymer toward Injectable Bioelectronics. *Chem. Mater.* **2022**, *34* (6), 2752−2763.
(52) Koutsouras, D. A.; Lingstedt, L. V.; Lieberth, K.; Reinholz, J.; Mailänder, V.; Blom, P. W. M.; Gkoupidenis, P. Probing the Impedance of a Biological Tissue with PEDOT:PSS-Coated Metal Electrodes: Effect of Electrode Size on Sensing Efficiency. *Adv. Healthcare Mater.* **2019**, *8* (23), 1901215.
(53) Pitsalidis, C.; Van Niekerk, D.; Moysidou, C. M.; Boys, A. J.; Withers, A.; Vallet, R.; Owens, R. M. Organic Electronic Transmembrane Device for Hosting and Monitoring 3D Cell Cultures. *Sci. Adv.* **2022**, *8*, No. eabo4761.
(54) Lu, Z.; van Niekerk, D.; Savva, A.; Kallitsis, K.; Thiburce, Q.; Salleo, A.; Pappa, A. M.; Owens, R. M. Understanding Electrochemical Properties of Supported Lipid Bilayers Interfaced with Organic Electronic Devices. *J. Mater. Chem. C* **2022**, *10* (20), 8050−8060.
(55) Savva, A.; Saez, J.; Withers, A.; Barberio, C.; Stoeger, V.; Elias-Kirma, S.; Lu, Z.; Moysidou, C. M.; Kallitsis, K.; Pitsalidis, C.; Owens, R. M. 3D Organic Bioelectronics for Electrical Monitoring of Human Adult Stem Cells. *Mater. Horiz.* **2023**, *10* (9), 3589−3600.
(56) Hopkins, J.; Fidanovski, K.; Travaglini, L.; Ta, D.; Hook, J.; Wagner, P.; Wagner, K.; Lauto, A.; Cazorla, C.; Officer, D.; Mawad, D. A Phosphonated Poly(Ethylenedioxythiophene) Derivative with Low Oxidation Potential for Energy-Efficient Bioelectronic Devices. *Chem. Mater.* **2022**, *34* (1), 140−151.
(57) Hopkins, J.; Ta, D.; Lauto, A.; Baker, C.; Daniels, J.; Wagner, P.; Wagner, K. K.; Kirby, N.; Cazorla, C.; Officer, D. L.; Mawad, D. Impact of Side Chain Extension on the Morphology and Electrochemistry of Phosphonated Poly(Ethylenedioxythiophene) Derivatives. *Adv. Mater. Technol.* **2023**, *8* (19), 2300777.
(58) Fenoy, G. E.; Azzaroni, O.; Knoll, W.; Marmisollé, W. A. Functionalization Strategies of PEDOT and PEDOT:PSS Films for Organic Bioelectronics Applications. *Chemosensors* **2021**, *9* (8), 212.
(59) Wustoni, S.; Hidalgo, T. C.; Hama, A.; Ohayon, D.; Savva, A.; Wei, N.; Wehbe, N.; Inal, S. In Situ Electrochemical Synthesis of a Conducting Polymer Composite for Multimetabolite Sensing. *Adv. Mater. Technol.* **2020**, *5* (3), 1900943.
(60) Ghazal, M.; Daher Mansour, M.; Scholaert, C.; Dargent, T.; Coffinier, Y.; Pecqueur, S.; Alibart, F. Bio-Inspired Adaptive Sensing through Electropolymerization of Organic Electrochemical Transistors. *Adv. Electron. Mater.* **2022**, *8* (3), 2100891.
(61) Lee, J.; Chhatre, S.; Sitarik, P.; Wu, Y.; Baugh, Q.; Martin, D. C. Electrochemical Fabrication and Characterization of Organic Electrochemical Transistors Using Poly (3, 4-Ethylenedioxythiophene) with Various Counterions. *ACS Appl. Mater. Interfaces* **2022**, *14* (37), 42289−42297.
(62) Nicolini, T.; Shinde, S.; El-Attar, R.; Salinas, G.; Thuau, D.; Abbas, M.; Raoux, M.; Lang, J.; Cloutet, E.; Kuhn, A. Fine-Tuning the Optoelectronic and Redox Properties of an Electropolymerized Thiophene Derivative for Highly Selective OECT-Based Zinc Detection. *Adv. Mater. Interfaces* **2024**, 2400127.
(63) Ji, J.; Fu, Y.; Wang, J.; Chen, P. Y.; Han, D.; Zhang, Q.; Zhang, W.; Sang, S.; Yang, X.; Cheng, Z. Bipolar Electrodeposition of Organic Electrochemical Transistor Arrays. *J. Mater. Chem. C* **2020**, *8* (33), 11499−11507.
(64) Schmidt, M. M.; ElMahmoudy, M.; Malliaras, G. G.; Inal, S.; Thelakkat, M. Smaller Counter Cation for Higher Transconductance in Anionic Conjugated Polyelectrolytes. *Macromol. Chem. Phys.* **2018**, *219* (2), 1700374.
(65) Musumeci, C.; Vagin, M.; Zeglio, E.; Ouyang, L.; Gabrielsson, R.; Inganäs, O. Organic Electrochemical Transistors from Supramolecular Complexes of Conjugated Polyelectrolyte PEDOTS. *J. Mater. Chem. C* **2019**, *7* (10), 2987−2993.
(66) Zeglio, E.; Schmidt, M. M.; Thelakkat, M.; Gabrielsson, R.; Solin, N.; Inganäs, O. Conjugated Polyelectrolyte Blends for Highly Stable Accumulation-Mode Electrochemical Transistors. *Chem. Mater.* **2017**, *29* (10), 4293−4300.
(67) Dubey, A.; Burke, N. A. D.; Stöver, H. D. H. Preparation and Characterization of Narrow Compositional Distribution Polyampholytes as Potential Biomaterials: Copolymers of N-(3-Aminopropyl)-Methacrylamide Hydrochloride (APM) and Methacrylic Acid (MAA). *J. Polym. Sci., Part A: Polym. Chem.* **2015**, *53* (2), 353−365.

https://doi.org/10.1021/acsami.4c03229
ACS Appl. Mater. Interfaces XXXX, XXX, XXX−XXX